Design and test of Wendelstein 7-X Water-cooled Divertor Scraper

J. Boscary, H. Greuner, G. Ehrke, B. Böswirth, Z. Wang, E. Clark, A. Lumsdaine, J. Tretter, P. Junghanns, R. Stadler, D. McGinnis, J. Lore, and The W7-X Team

Abstract— **Heat load calculations have indicated the possible overloading of the ends of the water-cooled divertor facing the pumping gap beyond their technological limit. The intention of the scraper is the interception of some of the plasma fluxes both upstream and downstream before they reach the divertor surface. The scraper is divided into six modules of four plasma facing components (PFCs); each module has four PFCs hydraulically connected in series by two water boxes (inlet and outlet). A full-scale prototype of one module has been manufactured. Development activities have been carried out to connect the water boxes to the cooling pipes of the PFCs by tungsten inert gas internal orbital welding. This prototype was successfully tested in the GLADIS facility with 17 MW/m2 for 500 cycles. The results of these activities have confirmed the possible technological basis for a fabrication of the water-cooled scraper.**

***Index Terms*— Stellarator; Wendelstein 7-X; Plasma Facing Component; Divertor; Scraper**

I. Introduction

The operation of the stellarator Wendelstein 7-X (W7-X) is divided into two consecutive phases. At first, an adiabatically loaded divertor [1] made of fine grain graphite tiles clamped onto a stainless steel support structure will be operated in 2016-2017 for a plasma duration up to 10 s with up to 8 MW input power. It will be then replaced by an actively water-cooled divertor designed for stationary plasma operation with a pulse length of up to 30 minutes with 10 MW input power and peak power with additional heating systems of up to 24 MW for 10 s [2]. Heat load calculations taking into account the effect of bootstrap current have indicated the possible overloading of the ends of the water-cooled divertor targets close to the pumping gap. These ends of the targets are designed for a maximal heat flux of 5MW/m² [3]. The possible overloading was revealed once the design of the divertor was finished and the divertor target elements in production. The intention of the additional scraper is the interception of some of the plasma fluxes both upstream and downstream before they reach the divertor surface. To study the effect of the scraper on the divertor for long-pulse operation, an uncooled scraper will be installed during the phase of the short pulse operation [4, 5].

Design activities have been carried out to prepare a possible fabrication of the water-cooled scraper for the second operation phase [6]. Full-scale prototypes have been manufactured and tested to validate the design and to develop required technologies.

II. Design of the Scraper

Fig. 1 shows the present design of the water-cooled scraper. Its toroidal and poloidal size are 692 and 360 mm, respectively. It is made of 24 identical plasma facing components (PFCs). A PFC is 247 mm long and 28 mm wide. It has 13 monoblocks made of carbon fibre reinforced carbon (CFC) NB31 bonded by hot isostatic pressing onto a CuCrZr cooling tube equipped with a copper twisted tape. Due to pressure drop and water feeding limitations, the scraper is divided into 6 modules of four PFCs hydraulically connected in series by 2 water boxes, one for the inlet and the other for the outlet. The six modules are fed in parallel from two manifolds located under the PFCs.

The plasma facing surface of the scraper has been shaped to limit the local heat flux to 20 MW/m². The integration of the scraper in a very limited available space required a compact design and in particular of the water boxes.

III. Scraper module prototype

The scraper is made of six similar modules which have different plasma facing surface shaping. The production of the prototype of one module will validate the production of the whole scraper. The first module on the right side highlighted in green in Fig. 1 has the most important curvature. This geometry has been selected because it is the most difficult in terms of tolerance achievement. Eight full-scale prototypes of PFCs were manufactured by the Austrian company PLANSEE SE.

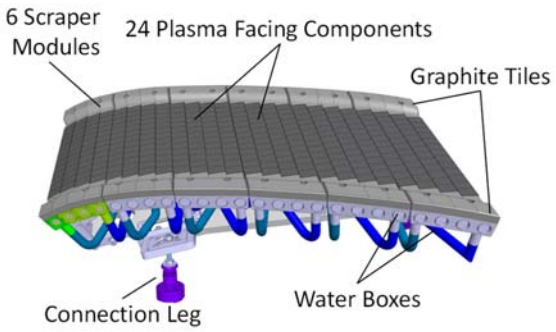

Fig. 1. View of the water-cooled divertor scraper to protect the divertor ends.

The CFC monoblock design and bonding technology were originally developed for ITER [7]. Four PFC prototypes were successfully tested and cycled in the high heat flux test facility GLADIS up to 20 MW/m² [8]. The applied water cooling conditions were: water velocity 12 m/s, 15 °C inlet temperature and 1 MPa static pressure. A twisted tape is installed inside the cooling pipe.

The design of the module prototype was simplified to focus on the technology for the fabrication of the water boxes (Fig. 2 and 5). The graphite tiles needed for shielding the water boxes (Fig. 1) are not included. The possible 3D machining of the individual PFC is not considered.

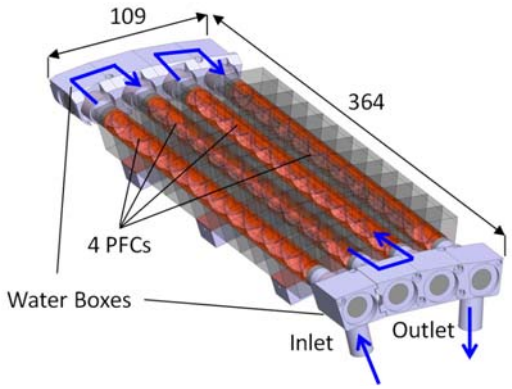

Fig. 2: View of the scraper module prototype. Monoblocks are transparent to show the twisted tape inside each of the cooling pipe (unit in mm).

The way of connecting the cooling pipe of the PFCs has defined the design of the water boxes. Due to access restrictions, the selected solution was the orbital welding from the inside. This technology was successfully applied in W7-X to the production of hundreds of manifolds for the cooling circuits of the first wall components and the water-cooled target modules of the divertor by the company Dockweiler [9]. The resulting design of the water boxes is shown in Fig. 3.

Due to the serial hydraulic arrangement of the PFCs (Fig. 2), the water box at the feeding side has to be split into two parts, which are welded together at the end. The water boxes need many apertures either for the channel machining or for the welding. Their size has to allow the installation and precise positioning of the welding tool as well as the visual inspection of the welds with a videoscope. To secure the fabrication of the prototype, an intermediate step was added with the manufacture of a demonstration prototype, replacing PFCs by stainless steel tubes.

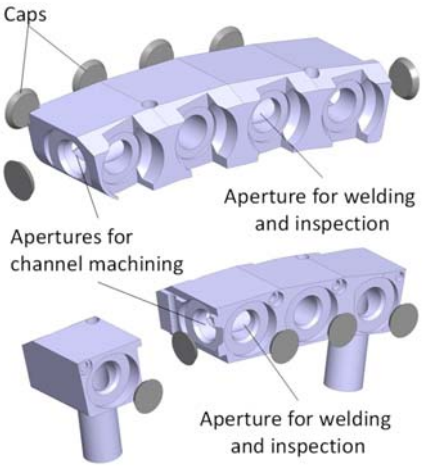

Fig. 3: View of the design of water boxes.

Fig. 4: Picture of the scraper module prototype (courtesy of Dockweiler).

The specification for the welds is full penetration without gaps, no discoloration. One challenge is to maintain the geometrical stability of a small component with a high number of weld seams. Many attempts with small probes have been necessary to produce the demonstration prototype mounted on the jig shown in Fig. 4. The tubes are firstly precisely positioned and spot welded at the outside to the water boxes to maintain their position. After welding from the inside, the caps are hand welded to close apertures.

This prototype passed the helium leak tightness test in oven with the following acceptance criteria: a leak rate lower than 5.10^{-7} Pa l/s at room temperature and 3.2 MPa internal He pressure, and a leak rate lower than 5.10^{-6} Pa l/s at 160°C and 2.8 MPa internal He pressure. The successful testing of the demonstration prototype released the manufacture of the module prototype. Fig. 5 shows the simulation of the positioning of the welding guns of the prototype placed on its jig.

Fig. 5 shows an evolution of the design of the jig with at the both ends an additional support for the water boxes to improve the geometrical accuracy of the module and the positioning of the welding gun. The position of the PFCs has to be guaranteed until the end of the welding process, to avoid the generation of larger steps between them which could lead to possible local overloading of the PFC edge. At the beginning, the position of the PFCs on the jig is measured with a robotic arm. The water boxes are spot welded to the PFCs and the PFC position is measured again.

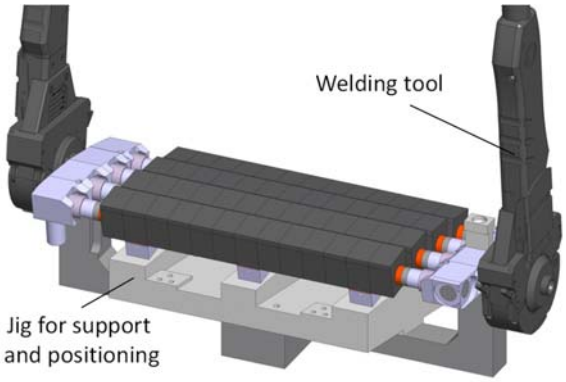

Fig. 5: Simulation of welding tool positioning for the module prototype.

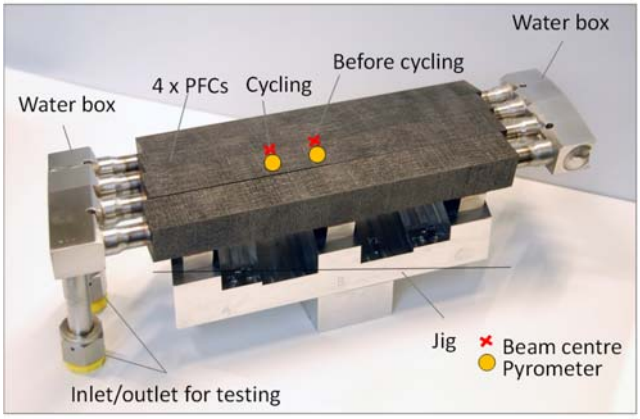

Fig. 6: Picture of the scraper module prototype

The welding gun is then positioned. The position of the welding head was particularly tricky to take into account the arc deflection due to the difference in the sulfur content between the end of the cooling pipe and the water box, both made of 316L [10]. During the welding, the pressure of gas

flushing (Ar) and the oxygen content is permanently measured to guarantee the weld quality. After each weld, a visual inspection with a video-scope is performed. The finished module prototype is shown in Fig. 6. This prototype also passed the helium leak tightness test in oven.

The issues for the welding did not allow optimizing the design of the channel of the water boxes from the hydraulic point of view. Fig. 7 shows the measured evolution of the pressure drop as a function of the flow rate.

The allowed pressure drop inside the plasma vessel is 1.8 MPa. The pressure drop at a velocity of 10.9 m/s (1.1 kg/s) is 1.4 MPa. The port for the water feeding of the scraper is not in the vicinity and a detailed analysis will be needed to check whether the remaining pressure is sufficient for this connection. In any case, this velocity can be considered as a first limit for operation.

IV. High Heat Flux Test Campaign

The campaign was carried out in the GLADIS facility, which generates a loading distribution with a Gaussian profile. The prototype was mounted outside the chamber onto a support frame and moved into the chamber with the manipulator of the vacuum lock system to be positioned normal to the beam axis in the vacuum chamber of the facility.

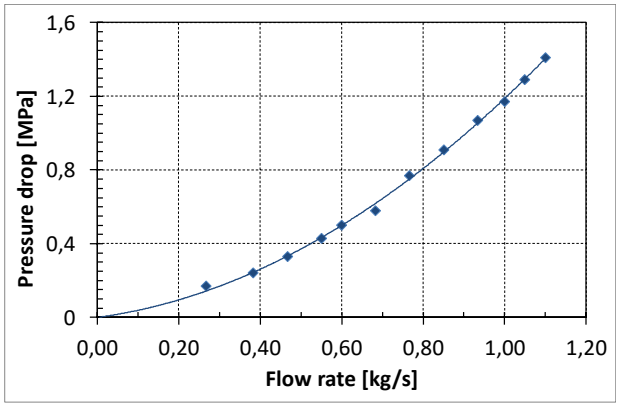

Fig. 7: Measurement of the pressure drop of the scraper module prototype.

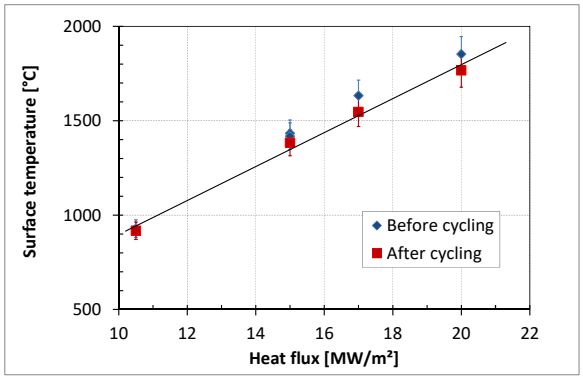

Fig. 8: Surface temperature measurement before and after cycling of the scraper module prototype. Note the slightly different measuring positions as indicated in Fig. 5. Values are given ± 5%.

Water-cooling conditions are: a flow rate is 1.07 kg/s, which corresponds to a velocity of 10.5 m/s in the cooling pipe of the PFCs, the inlet temperature is room temperature, the static pressure is 1 MPa. The duty cycle is 15 s. on and 60 s. off. A screening test with increasing the heat flux (10.5, 15, 17, 20 MW/m²) was performed before and after cycling. Fig. 8 shows the measurement of the surface temperature before and after cycling made with a one color pyrometer. The temperature is an averaged temperature measured within a spot size of 20 mm by the pyrometer. In case of CFC this measurement is difficult because the surface is a mixture of fibres and matrix with locally very different heat conductivities. A CFC emissivity of 0.8 was assumed for the pyrometer. The position of the spot measurement of the pyrometer on the prototype is indicated in Fig. 6.

A Gaussian heat flux profile with 17 MW/m² central heat flux and 150 mm full width of half maximum was applied for the cycling tests to limit the maximal surface temperature to < 1600°C. This profile was directly measured in front of the prototype. The scatter of the operation parameter is ± 5%. Fig. 9 shows that the evolution of the surface temperature measured by a one color pyrometer was stable during 500 cycles.

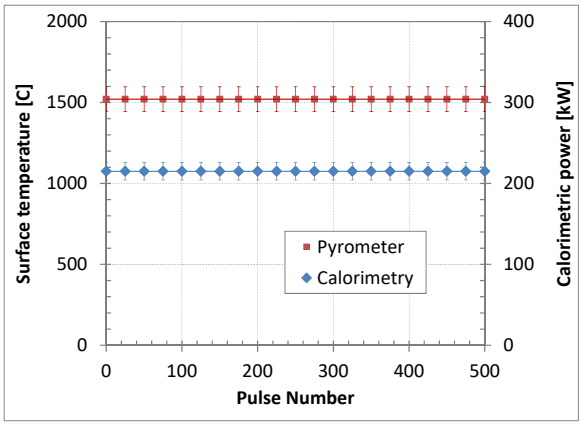

Fig. 9: Evolution of the surface temperature compared to the calorimetrically measured heat load during cycling with 17 MW/m². Values are given ± 5%.

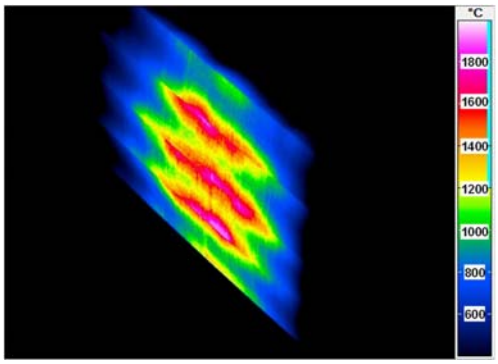

Fig. 10: Picture of the infrared image in the thermal equilibrium of the loaded surface of the scraper module prototype at 17 MW/m². Flow direction is indicated in Fig. 2.

Fig. 11: Picture of the loaded surface of the scraper module prototype after high heat flux cycling and screening tests in GLADIS.

The surface temperature distribution of the module prototype in the infrared range taken during cycling for 17 MW/m² is shown in Fig. 10.

The surface temperature distribution of the four PFCs appears not to be uniform. The monoblock geometry always induces a thermal gradient between the outer edges and the centre of the CFC blocks. A misalignment in the orientation of the carbon fiber mesh during production of the CFC results in further asymmetries of the surface temperature [12], [13]. Therefore, the resulting surface temperature distribution is not uniform as expected from the Gaussian distributed heat load. However, the screening test performed after cycling (Fig. 6) confirmed the stable performance of the prototype. Some differences of the temperature measurements between before and after cycling are due to the change of the position of the beam centre; the shield protecting one of the water boxes started to melt. Visual inspection and He-leak tightness test confirmed no degradation of the prototype after cycling. Fig. 9 shows the surface of the module prototype at the end of the high heat flux testing. The loaded surface is clearly visible.

V. Conclusion

The aim of the water-cooled scraper is to protect the ends of the actively cooled divertor for the phase of operation with plasma pulse duration up to 30 min. Its integration in the plasma vessel required a very compact design for the cooling system to remove localized heat fluxes as high as 20 MW/m² in steady state conditions.

The scraper has six similar modules. A scraper module is a set of four PFCs and two water boxes (inlet, outlet). Due to the restricted available space, the tungsten inert gas welding technology from the inside has been selected to connect the cooling pipe of the PFCs to the water boxes. The manufactured prototype has been successfully tested; no degradation of the performance was detected after 500 cycles with a heat flux of 17 MW/m². It was confirmed by the leak tightness test with pressurized helium performed in oven. The results of these activities have defined the possible technological basis for a fabrication of the water-cooled scraper.

References

[1] A. Peacock, *et al.,* "Progress in the design and development of a test divertor (TDU) for the start of W7-X operation", *Fusion Eng. Des.,* vol. 84, pp. 1475-1478, Jun 2009.

[2] R. C. Wolf, *et al.*, "Wendelstein 7-X Program – Demonstration of a Stellarator Option for Fusion Energy", I*EEE Trans. on Plasma Sci.,*vol. 44, no. 9, pp. 1466-1471, Sep. 2016.

[3] J. Boscary, *et al.,* "Design improvement of the target elements of Wendelstein 7-X divertor," *Fusion Eng. Des.,* vol. 87, pp. 1453-1456, Aug. 2012.

[4] A. Lumsdaine, *et al.,* "Overview of Activities for the Wendelstein 7-X Scraper Element Collaboration," *in Proc. IEEE 26th SOFE*, May 2015.

[5] J. Fellinger, *et al.,* "Integration of Uncooled Scraper Elements and its Diagnostics into Wendelstein 7-X," *Fusion Eng. Des.,* vol. 124, pp. 226-230, Nov. 2017.

[6] J. Boscary, *et al.,* "Development activities of the high heat flux scraper element," *Fusion Eng. Des.,* vols. 98-99, pp. 1231-1234, Oct. 2015.

[7] M. Richou, *et al.,* "Assessment of CFC grades under thermal fatigue for the ITER inner vertical target," *Phys. Scripta,* vol. T145, p.014082, Dec. 2011.

[8] H. Greuner et al., "High heat flux facility GLADIS: Operational characteristics and results of W7-X pre-series target tests", *J. Nuclear Mater.,* vols. 367–370, pp. 1444-1448, Aug. 2007.

[9] J. Boscary, *et al.*, "Prototyping phase of the high heat flux scraper element of Wendelstein 7-X," *Fusion Eng. Des.,* vols. 109-111, pp. 773-776, Nov. 2016.

[10] B. Mendelevitch, *et al.,* "Design analysis and manufacturing of the cooling lines of the in vessel components of W7-X," *Fusion Eng. Des.,* vol. 86, pp. 1669–1672, Oct. 2011.

[11] J. L. Fihey, R. Simoneau, "Weld penetration variation in GTA welding of some 304L stainless steels," presented at the Amer. Welding Soc. Conf., Kansa City, MO, USA, 1982.

[12] E. Clark *et al.*, "Thermal-Hydraulics Modeling for Prototype Testing of the W7-X High Heat Flux Scraper Element," *Fusion Eng. Des.,* vol. 121, pp. 211-217, Oct. 2017.

[13] J. Boscary et al., "Fabrication and testing of W7-X pre-series target elements," *Phys. Scripta,* vol. T128, pp. 195-199, Mar 2007.